MTLA 27 (2023) 101708

Contents lists available at ScienceDirect

Materialia

journal homepage: www.elsevier.com/locate/mtla

Reconciling experimental and theoretical stacking fault energies in *face-centered cubic* materials with the experimental twinning stress

Konstantin V. Werner [a,*], Frank Niessen [a], Wei Li [b,c], Song Lu [b], Levente Vitos [b,c,d], Matteo Villa [a], Marcel A.J. Somers [a]

[a] Department of Civil and Mechanical Engineering, Technical University of Denmark, Produktionstorvet, Building 425, Kongens, Lyngby 2800, Denmark
[b] Applied Materials Physics, Department of Materials Science and Engineering, Royal Institute of Technology, Stockholm SE-100 44, Sweden
[c] Department of Physics and Astronomy, Division of Materials Theory, Uppsala University, P.O. Box 516, Uppsala SE-75121, Sweden
[d] Research Institute for Solid State Physics and Optics, Wigner Research Center for Physics, P.O. Box 49, Budapest H-1525, Hungary

ARTICLE INFO

Keywords:
Metastable phases
Stacking fault energy
Twinning
Density functional theory

ABSTRACT

Stacking fault energy and twinning stress are thought to be closely correlated. All currently available models predict a monotonous decrease in twinning stress with decreasing stacking fault energy and depart from the assumption that the intrinsic stacking fault energy has a positive value. Opposite to this prediction, for medium- and high-entropy alloys the twinning stress was shown to increase with decreasing SFE. Additionally, for metastable materials, first principles methods predict negative intrinsic stacking fault energy values, whilst experimentally determined values are always positive. In the present communication, it is postulated that the twinning stress scaled by the Burgers vector bridges the difference between intrinsic and experimentally measured stacking fault energy. The assumption is tested for Cu-Al alloys, for pure metals and for medium- and high-entropy alloys and, for the first time, provides a consistent quantitative interpretation of data for both alloys with positive and negative stacking fault energy.

1. Introduction

The stacking fault energy (SFE) is the energy associated with a stacking fault (SF) bound by a leading and a trailing Shockley partial dislocation, that result from the dissociation of a full dislocation. In *face-centered cubic* (fcc) alloys, SFE is assumed to determine the predominant plastic deformation mechanism. In dependence on temperature and pressure, the SFE of alloys can be tailored by changing the chemical composition [1–4]. For increasing SFE, the prevalent deformation mechanism changes from martensite formation to deformation twinning to, exclusively, dislocation slip [5–7].

Experimentally, SFE values are assessed from transmission electron microscopy (TEM) observations of Shockley partial dislocation configurations, e.g. in extended dislocation nodes [8], SF tetrahedra [9], and from the separation between two Shockley partial dislocations, i.e. the SF width, by strong beam [10] and weak beam dark-field imaging (WBDF) [11]. Occasionally, high-resolution transmission electron microscopy (HRTEM) is applied [12]. Other frequently applied methods, e.g. X-ray and neutron diffraction do not enable direct assessment of SFE values [13], but are calibrated relying on TEM results.

Following the correlation of SFE and prevalent deformation mechanisms in *fcc* materials, Eqs. (1)–(4) in Table 1 were proposed to interrelate experimentally determined SFE values and the experimentally determined critical resolved shear stress for twinning (τ_{Twin}). Models proposed by Narita and Takamura [14] and Byun [15] conceive the experimentally determined SFE as an intrinsic materials property and predict a monotonous decrease of τ_{Twin} with decreasing SFE. The tendency of a material to undergo deformation twinning is also influenced by the microstructure. Smaller grains require a higher critical resolved shear stress to form deformation twins [16,17], while in ultra-fine grains twinning is fully suppressed [18]. Accordingly, Gutierrez-Urrutia et al. [19] and Meyers et al. [20] extended Byun's work to include the influence of grain size (Eqs. (3) and (4) in Table 1).

Saka et al. and Lee and Choi previously pointed out that experimentally determined SFE values should be considered "apparent" as they may be affected by other factors than chemical composition [21–23]. Müllner and Ferreira [24] ascribed the differences between experimentally determined and intrinsic (as modelled based on

* Corresponding author.
E-mail address: kviwe@mek.dtu.dk (K.V. Werner).

https://doi.org/10.1016/j.mtla.2023.101708
Received 23 January 2023; Accepted 4 February 2023
Available online 6 February 2023

Table 1
Models describing the relation of the critical resolved shear stress for twinning with the SFE obtained via experiments.

Reference	Critical resolved shear stress for twinning, τ_{Twin}
Grain size independent models	
Narita and Takamura [14]	$\tau_{Twin} = \frac{\gamma_{isf}^{exp}}{2b_p}$ (1)
Byun [15]	$\tau_{Twin} = \frac{2\gamma_{isf}^{exp}}{b_p}$ (2)
Grain size dependent models	
Gutierrez-Urrutia et al. [19]	$\tau_{Twin} = \frac{\gamma_{isf}^{exp}}{b_p} + \frac{\mu b_p}{D}$ (3)
Meyers et al. [20]	$\tau_{Twin} = \frac{\gamma_{isf}^{exp}}{b_p} + \frac{K_{Twin}^{HP}}{\sqrt{D}}$ (4)

composition) SFE values to strain energy from a difference in specific volume between *fcc* and the double-layer *hcp*, accounting to 1–4 $mJ{\cdot}m^{-2}$. However, results by Pierce et al. [25] show that strain energy alone cannot account for the observed discrepancy. Also Sun et al. [26] observed that the strain energy contribution is negligible compared to the observed discrepancies and suggested that these originate from a frictional force experienced by moving Shockley partial dislocations, thereby effectively altering the force balance over the stacking fault during its formation. Molecular dynamics simulations by Shih et al. [27] confirmed that solute-dislocation interactions result in a frictional force that is contained in experimental SFE values but is not accounted for in SFE values determined by applying Density Functional Theory (DFT).

We recently demonstrated for metastable fcc alloys, that satisfactory consistency is obtained between theoretical intrinsic and experimentally determined SFE values after proper correction [28]. *Experimental* SFE values do not represent an intrinsic materials property, as presupposed by the models in Table 1; the established theories thus need re-evaluation. In the present communication, it is postulated that the difference between experimental SFE values, γ_{isf}^{exp}, and SFE values predicted with DFT, γ_{isf}^{DFT}, is proportional to τ_{Twin}. Accordingly, the resistance experienced by moving Shockley partials that is omitted in a theoretical evaluation, is pragmatically accounted for.

2. Methodology

SFE values for *fcc* metals and $Cu_{100-x}Al_x$ binary alloys were calculated at room temperature with DFT [29,30] using the coherent potential approximation [31,32] as implemented in the exact muffin-tin orbitals package (EMTO) [32,33]. The *fcc* lattice was modelled using nine (111) layers containing one atom each and stacked in the standard sequence *ABCABCABC*. The lattice vectors of the *fcc* cell were $a_1 = a_0\langle 101\rangle/2$, $a_2 = a_0\langle 011\rangle/2$ and $a_3 = a_0\sqrt{3}\langle 111\rangle/3$, where a_0 is the *fcc* lattice parameter. Shifting a_3 by $a_0\langle 11\bar{2}\rangle/6$ introduced an intrinsic stacking fault via the periodic boundary condition, resulting in the new stacking sequence *ABCABCABC | BCABC …* [34]. The interplanar distance at the stacking fault interface was relaxed along a_3. The stacking fault energy was obtained from:

$$\gamma_{isf}^{DFT} = \left(F_{SF} - F_{fcc}\right)\Big/A \quad (5)$$

where F_{fcc} and F_{SF} are the Helmholtz energies of the supercells before and after introducing a SF of area A. The Helmholtz energies at room temperature were approximated by the total energies from first-principles calculations for atomic volumes derived from the experimental lattice parameters at room temperature. Unit cell volumes of the $Cu_{100-x}Al_x$ binary alloys were determined using Végard's law [35]. For Ni, spin-polarized calculations were performed [36]. The exchange-correlation functional was approximated using the Perdew, Burke, and Ernzerhof generalized gradient approximation [37]. The resolution of the k-point mesh was tested for energy convergence and consisted of 10,556 uniformly distributed points with an error of < 0.1 $mJ{\cdot}m^{-2}$ in SFE. DFT does not account for the strain fields associated with the Shockley partials.

Table 2
DFT calculated SFE values for pure Ag, Au, Cu, Al and Ni in comparison with calculated literature values [38–43].

Reference	γ_{isf}^{DFT} $mJ{\cdot}m^{-2}$				
	Ag	Au	Cu	Al	Ni
This work	25.0	40.0	48.8	116.5	155.7
Li et al. [38]	17.3	32.7	47.5	117.5	153.6
Zhang et al. [39]	–	–	38	110	110
Li et al. [40]	17	31	47	107	153
Kibey et al. [41]	18	33	41	130	110
Liu et al. [42]	–	–	38	134	120
Jin et al. [43]	16	25	36	112	133
Mean value	18.7 ± 3.6	32.3 ± 5.4	42.3 ± 5.3	118.1 ± 10.2	133.6 ± 20.7

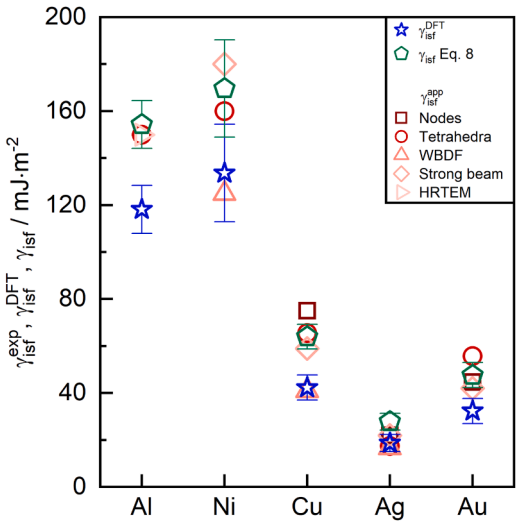

Fig. 1. Experimental SFE values, γ_{isf}^{exp} averaged over the respective techniques for pure Ag [10,44–46,56–62], Au [9,10,59,61] Cu [10,44,48,49,59,61,66], Al [12,59], Ni [10,54,55], in comparison with the mean DFT based SFE values [38–43], γ_{isf}^{DFT}, and the SFE values, γ_{isf}, calculated according to Eq. (8). Presentation in order of atomic number.

3. Results and discussion

SFE values for pure Ag, Au, Cu, Al, and Ni at 293 K as calculated with DFT (γ_{isf}^{DFT}) are given in Table 2 and are compared to calculated values reported in literature [38–43]. Only for Ni, a significant variation is observed among the calculated values, depending on how (well) ferromagnetism is accounted for.

Fig. 1 shows that experimentally determined SFE values, (γ_{isf}^{exp}) [9,10,12,44–62] are systematically higher than DFT predicted values, with exception of the values determined by WBDF imaging for Cu [44] and Ni [47]. In these cases, good agreement is observed, despite the dependence of γ_{isf}^{exp} values derived from WBDF images on the description of the dislocation core [44]. In particular for high-SFE materials such as Cu and Ni, where the separation distance between the two Shockley partial dislocations is small, SFE values derived from WBDF images are subject to systematic errors [44,63–65]. The results in Fig. 1 suggest that the applicability of WBDF imaging for SFE determination, is sensitive to the materials SFE itself.

The difference between DFT and experimental SFE values was

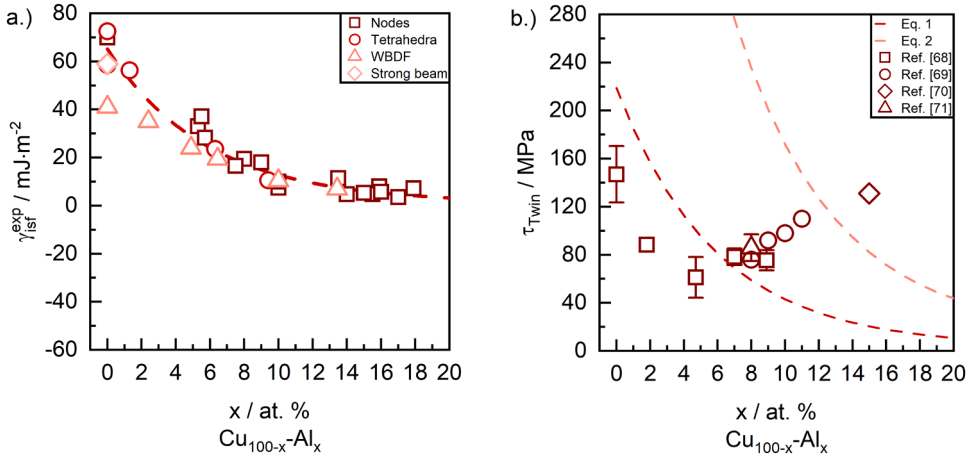

Fig. 2. a.) Experimental SFE values as a function of the Al-content in Cu-Al alloys determined from nodes [49,50,66,68–71], tetrahedra [9,59,61], WBDF [11,47] and strong beam [10] imaging, b.) Experimental critical resolved shear stresses for twinning [72–75] compared with τ_{Twin} predicted by the models by Narita and Takamura (Eq. (1)) and Byun (Eq. (2)). Note that the experimental τ_{Twin} values are, apart from the value by Tian et al. [74], determined on single crystalline alloys.

previously addressed for *metastable fcc* materials and ascribed to an incomplete definition of the force balance over a SF, as it assumes that Shockley partial dislocations can move freely in their glide plane [26,28,67]. The results presented in Fig. 1 suggest that the incomplete definition of the force balance also applies for *stable fcc* materials.

Experimental SFE values, γ_{isf}^{exp}, for a series of Cu-Al alloys are collected in Fig. 2a. For the compositional range considered, the alloy stability ranges from *stable* to *metastable*. Up to approximately 8 at.% Al, γ_{isf}^{exp} decreases almost linearly with Al-content and, eventually, asymptotically approaches 5 mJ·m^{-2}. For relatively low Al-contents, SFE values from WBDF are systematically lower than experimental SFE values from other techniques, analogous to pure metals. For higher Al-contents, experimental SFE values determined with WBDF coincide with SFE values determined from SF nodes and tetrahedra.

The critical resolved shear stress for twinning, τ_{Twin}, was calculated in dependence of the Al-content with the models in Eqs. (1) and (2) and is compared with experimental values from Refs. [72–75] in Fig. 2b.[1] Neither Eq. (1) nor Eq. (2) can accurately describe the dependence of experimental τ_{Twin} data on Al-content, indicating that γ_{isf}^{exp} alone is insufficient to describe the critical resolved shear stress for twinning τ_{Twin}.

As recently demonstrated, experimentally determined SFE values consist of a material's intrinsic SFE, γ_{isf}, and an excess term, γ^*, which accounts for the resistance experienced by moving Shockley partials in their common glide plane [28]:

$$\gamma_{isf}^{exp} = \gamma_{isf} + \gamma^* \tag{6}$$

γ^* was previously introduced by Sun et al. [26] to represent the discrepancy between the SFE determined by DFT, γ_{isf}^{DFT}, and γ_{isf}^{exp}, suggesting that γ_{isf} directly corresponds to γ_{isf}^{DFT} within computational accuracy. Including γ^* in the energy balance over a SF reconciles experimental SFE values, γ_{isf}^{exp}, for *metastable* alloys with negative SFE values from DFT [28]. Recognizing that an array of Shockley partials in *fcc* is equivalent to a coherent twin boundary, the resistance experienced by moving Shockley partial dislocations was pragmatically postulated to be proportional to the critical resolved shear stress for twinning, τ_{Twin} [28]:

$$\gamma^* = b_p \tau_{Twin} \tag{7}$$

with b_p the length of the Burgers vector of the partial dislocations. Rearranging Eqs. (6) and (7), τ_{Twin} relates to the SFE as:

$$\tau_{Twin} = \frac{\gamma^*}{b_p} = \frac{\gamma_{isf}^{exp} - \gamma_{isf}}{b_p} \tag{8}$$

Evidently, instead of just proportional to γ_{isf}^{exp} as in Eqs. (1)–(4) in Table 1, it is argued that τ_{Twin} is proportional to the excess term γ^*, which also accounts for grain size dependence [19]. Experimental SFE values of Cu-Al alloys (Fig. 2a) are compared with DFT values in Fig. 3a. Instead of the asymptotic approach to 5 mJ·m^{-2} observed for the experimental values, DFT predicts a continuous reduction in SFE with Al-content, from a positive to a negative value, in agreement with Ref. [40]. Accordingly, the observed asymptotic behavior of γ_{isf}^{exp} is interpreted as caused by the bias that experimental SFE values are always positive, owing to an incomplete definition of the energy balance over a SF [26,28,67]. Applying Eq. (8) and assuming $\gamma_{isf} = \gamma_{isf}^{DFT}$, the difference between the fitted (dashed) lines, as marked by the shaded area in Fig. 3a, divided by the Burgers vector $b_p = 0.149$ nm yields τ_{Twin} in dependence of Al-content. The critical resolved shear stress for twinning calculated with Eq. (8) is compared with experimental data for the twinning shear stress in Fig. 3b. Evidently, the calculated values for τ_{Twin} describe the dependence of independent experimental values for τ_{Twin} on Al-content with unprecedented quantitative accuracy. The systematic underestimate of τ_{Twin} could be as a result of a slight overestimation of γ_{isf}^{DFT} in this work. In this respect, it is noted that γ_{isf}^{DFT} values for Cu-Al alloys reported by Li et al. [40] are systematically 3–5 mJ·m^{-2} lower, which

[1] Note that the reported values for τ_{Twin} in Fig. 2b differ from the values reported by Venables (cf. Table 1 in Ref. [72]) due to the following reasons. At first, Venables established the observation of twins in TEM micrographs as a criterion to determine the twinning stress and calculated τ_{Twin} as the average of the lowest stress at which twins could be observed and the highest stress at which twins were still absent. For the Cu-Al alloy with 4.7 at. % Venables calculated τ_{Twin} as the average of data points showing small amounts of twins and twinning with load drops, whereas for alloys with 8.9 and 14.9 at. % Al Venables calculated τ_{Twin} as the average stress of the lowest stress at which stacking faults could be observed and the highest stress at which no stacking faults were observed. However, Tian et al. [74] have shown that in a Cu-15Al alloy stacking faults could already be observed at a plastic strain of 2 %, while twins were first discernable in TEM micrographs at significantly higher strains/stresses. This illustrates that at least in the case of Cu-Al alloys of low SFE, the twinning stress should not be determined based on the observation of stacking faults. Instead, as done in this work, the actual necessary shear stress for the formation of twins should be approximated by taking the mean value of the lowest stress values in Fig. 3 in Ref. [72] for which twinning is observed. Accordingly determined twinning stresses coincide with results from Szczerba & Szczerba [73] and Mori et al. [75] (cf. Fig. 3).

corresponds, according to Eq. (8), to a difference of 20–30 MPa in the twinning stress. The calculated γ_{isf}^{DFT} values in Fig. 3a provide an explanation as to why Eq. (1) provides reasonable τ_{Twin} values for Al-contents in the range 8–10 at.% (see Fig. 2b). For $\gamma_{isf} = 0$ mJ·m^{-2}, the experimental SFE value γ_{isf}^{exp} becomes equal to γ^* (see Eq. (7)). Accordingly, for materials with a small, positive or negative γ_{isf} it may appear that τ_{Twin} correlates with γ_{isf}^{exp}.

The trends in Fig. 3b are confirmed by the results of Tranchant et al. [76], who reported that the dependence of τ_{Twin} on Al-content can be divided into two subranges: i) for $\gamma_{isf}^{exp} > 17$ mJ·m^{-2}, i.e. < 9 at.% Al, τ_{Twin} decreases with decreasing γ_{isf}^{exp}; ii) for $\gamma_{isf}^{exp} > 17$ mJ·m^{-2}, i.e. > 9 at.% Al, τ_{Twin} increases with decreasing SFE. The non-monotonic dependence of τ_{Twin} on γ_{isf}^{exp} is explained from the transition from nucleation-controlled twinning for $\gamma_{isf}^{exp} > 17$ mJ·m^{-2} to propagation controlled twinning for $\gamma_{isf}^{exp} < 17$ mJ·m^{-2}. Twinning controlled by nucleation and growth/propagation is consistent with the current opinion on deformation twinning [20,77]. In the Cu-Al system the transition coincides with a change from positive to negative γ_{isf}^{DFT} values, i.e. transition from *stable* to *metastable fcc*. From a thermodynamics point of view the transition is logical. For a positive SFE, additional driving force by mechanical work must be introduced to nucleate twins in the *stable fcc* matrix. Once formed, these twins can easily extend by the propagation of Shockley partial dislocations. For negative SFE, the nucleation of SFs and twins in the *metastable fcc* matrix is thermodynamically favorable. Nevertheless, twins and wide SFs are first observed above τ_{Twin}, indicating that the propagation of Shockley partial dislocations is hindered. If twinning or SF formation would be nucleation-controlled, *metastable fcc* materials would readily twin or transform into martensite and thus be *unstable*, which, inherent to their *metastability*, is not observed.

In Fig. 4, Eq. (8) is applied to various *stable* and *metastable fcc* alloys to test general applicability. Convincingly, a linear relationship between τ_{Twin} and excess SFE γ^* is obtained over a wide range of τ_{Twin} values, consistent with Eq. (8). Li et al. [78] previously observed that the established models in Table 1 cannot be used to predict the trend of τ_{Twin} for *fcc* medium- (MEAs) and high-entropy alloys (HEAs). Notably, Eq. (8) consistently predicts that τ_{Twin} decreases in the order CoCrNi, CoCrFeNi to CoCrFeMnNi with increasing γ_{isf}^{exp}, whilst Eqs. (1)–(4) predict the opposite order.

In the presented framework, Eq. (8) enables calculation of the twinning stress from γ^* which requires that values for γ_{isf}^{exp} and γ_{isf}^{DFT} are available. Alternatively, the experimental SFE value can be calculated if τ_{Twin} and γ_{isf}^{DFT} are known. Thus, based on the average γ_{isf}^{DFT} values in Table 1 and the twinning stress values in Table 3, the "experimental" SFE values of pure metals were calculated with Eq. (8) and are given in Table 3. These predicted SFE values are also given in Fig. 1 and are in excellent agreement with the average experimentally determined γ_{isf}^{exp} data. The consistency between predicted and experimental γ_{isf}^{exp} values strongly supports the applicability of the postulate formulated in Eq. (8).

Finally, for most alloy systems, γ_{isf}^{exp} is reported to be temperature-dependent and decreases with decreasing temperature [87,88]. Consequently, Eqs. (1)–(4) would predict that τ_{Twin} decreases with decreasing temperature [89], which is in disagreement with experimental observations of a nearly temperature-independent τ_{Twin} [14,20,80,85,86,89]. Neding et al. [90] demonstrated that γ_{isf}^{exp} and γ_{isf}^{DFT} have the same temperature dependence within experimental and computational accuracy. Hence, the difference between experimental and theoretical SFE values, γ^*, is in this case constant. Thus, τ_{Twin} calculated according to Eq. (8) is temperature independent, in agreement with experimental

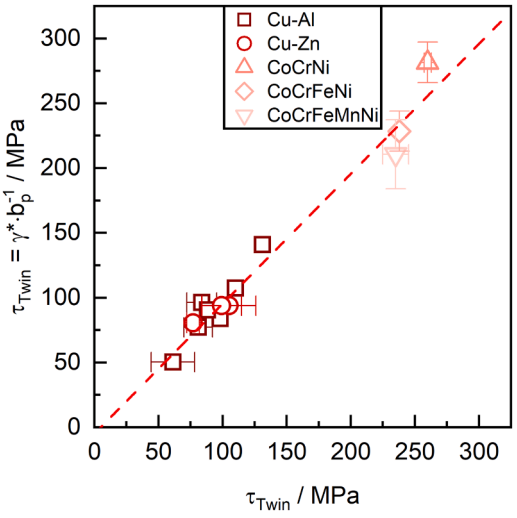

Fig. 4. Twinning stress values calculated according to Eq. (8) from apparent SFE values and SFE values predicted by DFT for Cu-Al (inferred from Fig. 3a), Cu-Zn [40,66], CoCrNi [26,79,80], CoCrFeNi [26,79,81] and CoCrFeMnNi [26,79,82] alloys as a function of the experimental twinning stress (τ_{Twin}) Cu-Al [72–75], Cu-Zn [83,84], CoCrNi [80], CoCrFeNi [81] and CoCrFeMnNi [85].

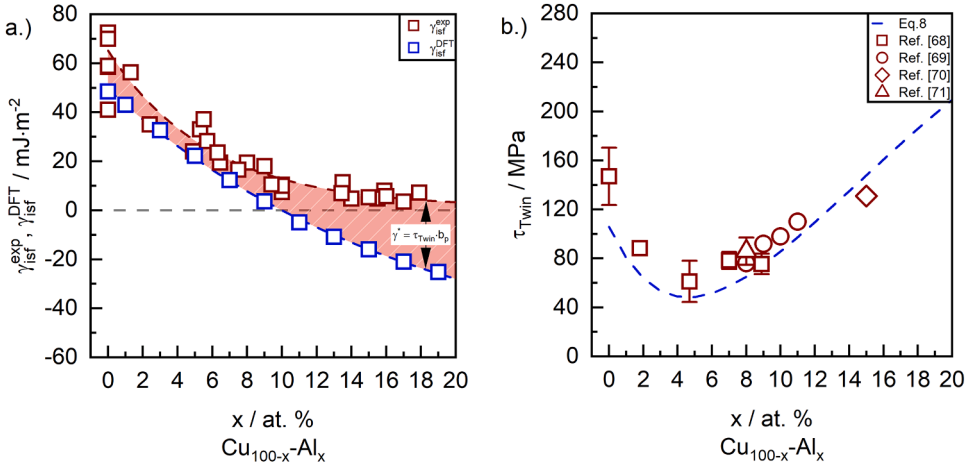

Fig. 3. a.) Experimental SFE values (γ_{isf}^{exp}) [9–11,47,49,50,59,61,66,68–71], and SFE values predicted by DFT (γ_{isf}^{DFT}) as a function of the Al-content in Cu-Al alloys, b.) Experimentally determined critical resolved shear stresses for twinning [72–75] and the predicted trend of τ_{Twin} in Cu-Al alloys according to Eq. (8). Note that the experimental τ_{Twin} values are, apart from the value by Tian et al. [74], determined on single crystalline alloys.

Table 3
Twinning stress τ_{Twin} of pure Ag, Au, Cu, Al and Ni together with apparent experimental SFE values predicted based on the average DFT values in Table 1 according to Eq. (8).

	Metal Ag	Au	Cu	Al	Ni
τ_{Twin} [MPa]	54.5 ± 16.5 [86]	92.5 ± 7.5 [86]	147 ± 23.5 [72]	220 [41]	250 [41]
γ_{isf}^{exp} [mJ·m^{-2}]	27.8 ± 3.6	47.6 ± 5.4	64.0 ± 5.3	154.4 ± 10.2	169.6 ± 20.7

observations.

Recently, a systematic discrepancy of -42 mJ·m^{-2} ($\gamma_{isf}^{exp} = 35 \pm 7$ mJ·m^{-2} and $\gamma_{isf}^{DFT} = -7$ mJ·m^{-2}) was reported between the experimental and DFT assessed SFE values for the equiatomic CrMn-FeCoNi HEA [91]. Applying Eq. (8), using $\tau_{Twin} = 235 \pm 20$ MPa [85] and $b_p = 1.47$ nm [91], shows that $\gamma^* = 35 \pm 2$ mJ·m^{-2}. Following the sum rule of uncertainties, Eq. (8) yields $\gamma_{isf} = 0 \pm 9$ mJ·m^{-2}, exemplifying that experimental and DFT assessed SFE values can be reconciled within experimental and computational accuracy. Further improvement of the agreement between experimental and theoretical SFE values could be achieved if, as suggested by Wagner et al. [91], vibrational, electronic, and magnetic excitations as well as atomic relaxations, were included in the calculations. Nevertheless, the discrepancy between experimental and theoretical SFE values appears to be largely bridged by the resistance experienced by moving Shockley partial dislocations $\gamma^* = b_p \tau_{Twin}$.

4. Conclusions

The discrepancy between DFT and experimental SFE values for pure metals as well as *stable* and *metastable fcc* alloys is reconciled by accounting for the critical resolved shear stress for twinning:

$$\gamma_{isf}^{exp} = \gamma_{isf}^{DFT} + b_p \tau_{Twin}$$

The equation expresses that experimentally determined SFE values are not an intrinsic materials property but depend on the path followed to introduce the stacking fault before observation. This path involves the movement of partial dislocations under the influence of a resolved shear stress and adds to the thermodynamically defined intrinsic stacking fault energy as calculated with DFT.

Applying the postulated equation to calculate the twinning stress for *fcc* metals as well as for stable and metastable *fcc* alloy systems from experimental and DFT SFE values, unprecedented quantitative agreement with experimentally determined twinning stresses is obtained. Furthermore, the calculated twinning stress is independent of temperature, consistent with experimental twinning stresses.

Declaration of Competing Interest

The authors declare that they have no known competing financial interests or personal relationships that could have appeared to influence the work reported in this paper.

Acknowledgments

This work was supported by the Independent Research Fund Denmark as part of the project SFETailor (Grant No. 9041–00145B). The authors would like to thank Francesco Maresca (University of Groningen) for the valuable scientific discussions.

References

[1] R.E. Schramm, R.P. Reed, Stacking fault energies of seven commercial austenitic stainless steels, Metall. Trans. A 6 (1975) 1345–1351, https://doi.org/10.1007/BF02641927.
[2] L. Vitos, J.O. Nilsson, B. Johansson, Alloying effects on the stacking fault energy in austenitic stainless steels from first-principles theory, Acta Mater. 54 (2006) 3821–3826, https://doi.org/10.1016/j.actamat.2006.04.013.
[3] T. Yonezawa, K. Suzuki, S. Ooki, A. Hashimoto, The effect of chemical composition and heat treatment conditions on stacking fault energy for Fe-Cr-Ni austenitic stainless steel, Metall. Mater. Trans. A Phys. Metall. Mater. Sci. 44 (2013) 5884–5896, https://doi.org/10.1007/s11661-013-1943-0.
[4] J.X. Yan, Z.J. Zhang, H. Yu, K.Q. Li, Q.M. Hu, J.B. Yang, Z.F. Zhang, Effects of pressure on the generalized stacking fault energy and twinning propensity of *face-centered cubic* metals, J. Alloys Compd. 866 (2021), 158869, https://doi.org/10.1016/j.jallcom.2021.158869.
[5] T.H. Lee, E. Shin, C.S. Oh, H.Y. Ha, S.J. Kim, Correlation between stacking fault energy and deformation microstructure in high-interstitial-alloyed austenitic steels, Acta Mater. 58 (2010) 3173–3186, https://doi.org/10.1016/j.actamat.2010.01.056.
[6] S. Allain, J.P.P. Chateau, O. Bouaziz, A physical model of the twinning-induced plasticity effect in a high manganese austenitic steel, Mater. Sci. Eng. A 387–389 (2004) 143–147, https://doi.org/10.1016/j.msea.2004.01.060.
[7] Y. Tian, O.I. Gorbatov, A. Borgenstam, A.V. Ruban, P. Hedström, Deformation microstructure and deformation-induced martensite in austenitic Fe-Cr-Ni alloys depending on stacking fault energy, Metall. Mater. Trans. A Phys. Metall. Mater. Sci. 48 (2017) 1–7, https://doi.org/10.1007/s11661-016-3839-2.
[8] M.J. Whelan, Dislocation interactions in face-centred cubic metals, with particular reference to stainless steel, Proc. R. Soc. London. Ser. A Math. Phys. Sci. 249 (1959) 114–137, https://doi.org/10.1098/rspa.1959.0011.
[9] M.H. Loretto, L.M. Clarebrough, R.L. Segall, Stacking-fault tetrahedra in deformed face-centred cubic metals, Philos. Mag. 11 (1965) 459–465, https://doi.org/10.1080/14786436508224233.
[10] F. Häussermann, M. Wilkens, Bestimmung der Stapelfehlerenergie kubisch-flächenzentrierter metalle aus der analyse des elektronenmikroskopischen beugungskontrastes von stapelfehlerdipolen, Phys. Status Solidi 18 (1966) 609–624, https://doi.org/10.1002/pssb.19660180214.
[11] D.J.H. Cockayne, I.L.F. Ray, M.J. Whelan, Investigations of dislocation strain fields using weak beams, Philos. Mag. 20 (1969) 1265–1270, https://doi.org/10.1080/14786436908228210.
[12] M.J. Mills, P. Stadelmann, M.J. Mills, A study of the structure of Lomer and 60 dislocations in aluminium using high-resolution transmission electron microscopy, Philos. Mag. A Phys. Condens. Matter. Struct. Defects Mech. Prop. 60 (1989) 355–384, https://doi.org/10.1080/01418618908213867.
[13] R.P. Reed, R.E. Schramm, Relationship between stacking-fault energy and x-ray measurements of stacking-fault probability and microstrain, J. Appl. Phys. 45 (1974) 4705–4711, https://doi.org/10.1063/1.1663122.
[14] N. Narita, J. Takamura, Deformation twinning in silver- and copper-alloy crystals, Philos. Mag. 29 (1974) 1001–1028, https://doi.org/10.1080/14786437408226586.
[15] T.S. Byun, On the stress dependence of partial dislocation separation and deformation microstructure in austenitic stainless steels, Acta Mater. 51 (2003) 3063–3071, https://doi.org/10.1016/S1359-6454(03)00117-4.
[16] Y.F. Shen, N. Jia, Y.D. Wang, X. Sun, L. Zuo, D. Raabe, Suppression of twinning and phase transformation in an ultrafine grained 2GPa strong metastable austenitic steel: experiment and simulation, Acta Mater. 97 (2015) 305–315, https://doi.org/10.1016/j.actamat.2015.06.053.
[17] J. Chen, F.T. Dong, Z.Y. Liu, G.D. Wang, Grain size dependence of twinning behaviors and resultant cryogenic impact toughness in high manganese austenitic steel, J. Mater. Res. Technol. 10 (2021) 175–187, https://doi.org/10.1016/j.jmrt.2020.12.030.
[18] S.J. Sun, Y.Z. Tian, H.R. Lin, H.J. Yang, X.G. Dong, Y.H. Wang, Z.F. Zhang, Transition of twinning behavior in CoCrFeMnNi high entropy alloy with grain refinement, Mater. Sci. Eng. A 712 (2018) 603–607, https://doi.org/10.1016/j.msea.2017.12.022.
[19] I. Gutierrez-Urrutia, S. Zaefferer, D. Raabe, The effect of grain size and grain orientation on deformation twinning in a Fe-22wt.% Mn-0.6wt.% C TWIP steel, Mater. Sci. Eng. A 527 (2010) 3552–3560, https://doi.org/10.1016/j.msea.2010.02.041.
[20] M.A. Meyers, O. Vöhringer, V.A. Lubarda, The onset of twinning in metals: a constitutive description, Acta Mater. 49 (2001) 4025–4039, https://doi.org/10.1016/S1359-6454(01)00300-7.
[21] Y. Lee, C. Choi, Driving Force for g → « Martensitic Transformation and SFE of austenite in Fe-Mn binary system, Metall. Mater. Trans. A 31A (2000) 355–360, https://doi.org/10.1007/s11661-000-0271-3.
[22] H. Saka, Y. Sueki, T. Imura, On the intrinsic temperature dependence of the stacking-fault energy in copper-aluminium alloys, Philos. Mag. A Phys. Condens. Matter. Struct. Defects Mech. Prop. 37 (1978) 273–289, https://doi.org/10.1080/01418617808235440.
[23] H. Saka, T. Kondo, T. Imura, The temperature dependence of the stacking-fault energy in silver-base alloys, Philos. Mag. A Phys. Condens. Matter. Struct. Defects Mech. Prop. 47 (1983) 859–868, https://doi.org/10.1080/01418618308243125.
[24] P. Mullner, P.J. Ferreira, On the energy of terminated stacking faults, Philos. Mag. Lett. 73 (1996) 289–298, https://doi.org/10.1080/095008396180551.
[25] D.T. Pierce, J.A. Jiménez, J. Bentley, D. Raabe, C. Oskay, J.E. Wittig, The influence of manganese content on the stacking fault and austenite/ε-martensite interfacial energies in Fe-Mn-(Al-Si) steels investigated by experiment and theory, Acta Mater. 68 (2014) 238–253, https://doi.org/10.1016/j.actamat.2014.01.001.
[26] X. Sun, S. Lu, R. Xie, X. An, W. Li, T. Zhang, C. Liang, X. Ding, Y. Wang, H. Zhang, L. Vitos, Can experiment determine the stacking fault energy of metastable alloys? Mater. Des. 199 (2021), 109396 https://doi.org/10.1016/j.matdes.2020.109396.

[27] M. Shih, J. Miao, M. Mills, M. Ghazisaeidi, Stacking fault energy in concentrated alloys, Nat. Commun. 12 (2021) 1–10, https://doi.org/10.1038/s41467-021-23860-z.

[28] K.V. Werner, F. Niessen, M. Villa, M.A.J. Somers, Experimental validation of negative stacking fault energies in metastable *face-centered cubic* materials, Appl. Phys. Lett. 119 (2021), 141902, https://doi.org/10.1063/5.0063761.

[29] W. Kohn, L.J. Sham, Self-consistent equations including exchange and correlation effects, Phys. Rev. 140 (1965) 1133–1138, https://doi.org/10.1103/PhysRev.140.A1133.

[30] P. Hohenberg, W. Kohn, Inhomogeneous electron gas, Phys. Rev. 136 (1964) 864–871, https://doi.org/10.1007/s12045-017-0529-3.

[31] P. Soven, Coherent-potential model of substitutional disordered alloys, Phys. Rev. 156 (1967) 809–813, https://doi.org/10.1103/PhysRev.156.809.

[32] L. Vitos, I.A. Abrikosov, B. Johansson, Anisotropic lattice distortions in random alloys from first-principles theory, Phys. Rev. Lett. 87 (2001), 156401–156401–4, https://doi.org/10.1103/PhysRevLett.87.156401.

[33] L. Vitos, Computational Quantum Mechanics For Materials Engineers - The EMTO Method and Applications, 1st ed., Springer, London, 2007 https://doi.org/10.1007/978-1-84628-951-4_5.

[34] W. Li, S. Lu, Q.M. Hu, B. Johansson, S.K. Kwon, M. Grehk, J.Y. Johnsson, L. Vitos, Generalized stacking fault energy of γ-Fe, Philos. Mag. 96 (2016) 524–541, https://doi.org/10.1080/14786435.2016.1140912.

[35] L. Vegard, Die konstitution der mischkristalle und die raumfüllung der atome, Z Für Phys. 5 (1921) 17–26, https://doi.org/10.1007/BF01349680.

[36] G. Grimvall, Spin disorder in paramagnetic fcc iron, Phys. Rev. B 39 (1989) 12300–12301, https://doi.org/10.1103/PhysRevB.39.12300.

[37] J.P. Perdew, K. Burke, M. Ernzerhof, Generalized gradient approximation made simple, Phys. Rev. Lett. 77 (1996) 3865–3868, https://doi.org/10.1103/PhysRevLett.77.3865.

[38] R. Li, S. Lu, D. Kim, S. Schönecker, J. Zhao, S.K. Kwon, L. Vitos, Stacking fault energy of *face-centered cubic* metals: thermodynamic and ab initio approaches, J. Phys. Condens. Matter. 28 (2016), 395001, https://doi.org/10.1088/0953-8984/28/39/395001.

[39] X. Zhang, B. Grabowski, F. Körmann, A.V. Ruban, Y. Gong, R.C. Reed, T. Hickel, J. Neugebauer, Temperature dependence of the stacking-fault Gibbs energy for Al, Cu, and Ni, Phys. Rev. B 98 (2018), 224106, https://doi.org/10.1103/PhysRevB.98.224106.

[40] W. Li, S. Lu, Q.M. Hu, S.K. Kwon, B. Johansson, L. Vitos, Generalized stacking fault energies of alloys, J. Phys. Condens. Matter. 26 (2014), 265005, https://doi.org/10.1088/0953-8984/26/26/265005.

[41] S. Kibey, J.B. Liu, D.D. Johnson, H. Sehitoglu, Predicting twinning stress in fcc metals: linking twin-energy pathways to twin nucleation, Acta Mater. 55 (2007) 6843–6851, https://doi.org/10.1016/j.actamat.2007.08.042.

[42] L. Liu, R. Wang, X. Wu, L. Gan, Q. Wei, Temperature effects on the generalized planar fault energies and twinnabilities of Al, Ni and Cu: first principles calculations, Comput. Mater. Sci. 88 (2014) 124–130, https://doi.org/10.1016/j.commatsci.2014.03.005.

[43] Z.H. Jin, S.T. Dunham, H. Gleiter, H. Hahn, P. Gumbsch, A universal scaling of planar fault energy barriers in *face-centered cubic* metals, Scr. Mater. 64 (2011) 605–608, https://doi.org/10.1016/J.SCRIPTAMAT.2010.11.033.

[44] D.J.H. Cockayne, M.L. Jenkins, I.L.F. Ray, The measurement of stacking-fault energies of pure face-centred cubic metals, Philos. Mag. 24 (1971) 1383–1392, https://doi.org/10.1080/14786437108217419.

[45] M.H. Loretto, L.M. Clarebrough, R.L. Segall, The stacking-fault energy of silver, Philos. Mag. 10 (1964) 731–732, https://doi.org/10.1080/14786436408228492.

[46] P.C.J. Gallagher, Stacking-fault energy in dilute silver alloys from extended node measurements, J. Appl. Phys. 39 (1968) 160–162, https://doi.org/10.1063/1.1655725.

[47] C.B. Carter, I.L.F. Ray, I.L.F Ray, On the stacking-fault energies of copper alloys, Philos. Mag. 35 (1977) 189–200, https://doi.org/10.1080/14786437708235982.

[48] L.F. Vassamillet, T.B. Massalski, Stacking fault probabilities of some alloys of copper and silver with zinc and cadmium, J. Appl. Phys. 34 (1963) 3398–3402, https://doi.org/10.1063/1.1729199.

[49] P.R. Thornton, T.E. Mitchell, P.B. Hirsch, The dependence of cross-slip on stacking-fault energy in face-centred cubic metals and alloys, Philos. Mag. 7 (1962) 1349–1369, https://doi.org/10.1080/14786436208213168.

[50] L.E. Murr, Relative interfacial free energy measurements in Cu and Cu-Al alloys, Phys. Status Solidi 3 (1970) 447–455, https://doi.org/10.1002/pssa.19700030219.

[51] M. Walter, L. Mujica Roncery, S. Weber, L. Leich, W. Theisen, XRD measurement of stacking fault energy of Cr–Ni austenitic steels: influence of temperature and alloying elements, J. Mater. Sci. 55 (2020) 13424–13437, https://doi.org/10.1007/s10853-020-04953-4.

[52] L.E. Murr, Temperature coefficient of twin-boundary energy: the determination of stacking-fault energy from the coherent twin-boundary energy in pure F.C.C. metals, Scr. Metall. 6 (1972) 203–208, https://doi.org/10.1016/0036-9748(72)90168-8.

[53] R.H. Rautioaho, An interatomic pair potential for aluminium calculation of stacking fault energy, Phys. Status Solidi 112 (1982) 83–89, https://doi.org/10.1002/pssb.2221120108.

[54] P. Humble, M.H. Loretto, L.M. Clarebrough, The nature of defects in quenched nickel, Philos. Mag. 15 (1967) 297–303, https://doi.org/10.1080/14786436708227702.

[55] C.B. Carter, S.M. Holmes, The stacking-fault energy of nickel, Philos. Mag. 35 (1977) 1161–1171, https://doi.org/10.1080/14786437708232942.

[56] P.C.J. Gallagher, J. Washburn, The stacking-fault energy in the Ag-In series, Philos. Mag. 14 (1966) 971–978, https://doi.org/10.1080/14786436608244768.

[57] A.W. Ruff, L.K. Ives, Dislocation node determinations of the stacking fault energy in silver-tin alloys, Acta Metall. 15 (1967) 189–198, https://doi.org/10.1016/0001-6160(67)90191-5.

[58] T.C. Tisone, R.C. Sundahl, G.Y. Chin, Stacking fault energy in noble metal alloys, Met Trans. 1 (1970) 1561–1567, https://doi.org/10.1007/bf02642001.

[59] T. Jøssang, J.P. Hirth, The energies of stacking-fault teirahedra in F.C.C. metals, Philos. Mag. 13 (1966) 657–670, https://doi.org/10.1080/14786436608212687.

[60] M. Wilkens, M. Rapp, K. Differt, Die Stapelfehlerenergie von silber verschiedener reinheit, Int. J. Mater. Res. 57 (1966) 746–750, https://doi.org/10.1515/ijmr-1966-571007.

[61] L.M. Clarebrough, P. Humble, M.H. Loretto, Faulted defects and stacking-fault energy, Can. J. Phys. 45 (1967) 1135–1146, https://doi.org/10.1139/p67-083.

[62] P.G.J. Gallagher, Y.C. Llu, The diversity of stacking fault energy determinations and its significance, Acta Metall. 17 (1969) 127–137, https://doi.org/10.1016/0001-6160(69)90133-3.

[63] D.J.H. Cockayne, V. Vitek, Effect of core structure on the determination of the stacking-fault energy in close-packed metals, Phys. Status Solidi 65 (1974) 751–764, https://doi.org/10.1002/pssb.2220650236.

[64] C.B. Carter, S.M. Holmes, The study of faulted dipoles in copper using weak-beam electron microscopy, Philos. Mag. 32 (1975) 599–614, https://doi.org/10.1080/14786437508220883.

[65] R.C. Perrin, E.J. Savino, Computer simulation of weak-beam images of extended dislocations in copper, J. Microsc. 98 (1973) 214–220, https://doi.org/10.1111/j.1365-2818.1973.tb03826.x.

[66] A. Howie, P.R. Swann, Direct measurements of stacking-fault energies from observations of dislocation nodes, Philos. Mag. 6 (1961) 1215–1226, https://doi.org/10.1080/14786436108243372.

[67] S. Wei, C.C. Tasan, Deformation faulting in a metastable CoCrNiW complex concentrated alloy: a case of negative intrinsic stacking fault energy? Acta Mater. 200 (2020) 992–1007, https://doi.org/10.1016/j.actamat.2020.09.056.

[68] P.C.J. Gallagher, The influence of alloying, temperature, and related effects on the stacking fault energy, Metall. Trans. 1 (1970) 2429–2461, https://doi.org/10.1007/BF03038370.

[69] T.C. Tisone, J.O. Brittain, M. Meshii, Stacking faults in a cu-15 at% al alloy. i. the short range order and temperature dependence of the stacking fault energy, Phys. Status Solidi 27 (1968) 185–194, https://doi.org/10.1002/pssb.19680270119.

[70] Y. Tomokiyo, K. Kaku, T. Eguchi, The influence of solute atoms on the stacking fault energy in and amp;alpha;cu and amp;ndash;al alloys, Trans. Japan Inst. Met. 15 (1974) 39–45, https://doi.org/10.2320/matertrans1960.15.39.

[71] K. Kamada, Effects of annealing and irradiation on the stacking-fault energy of CuSingle Bond signAl solid solutions, J. Appl. Phys. 39 (1968) 1824–1828, https://doi.org/10.1063/1.1656437.

[72] J.A. Venables, The electron microscopy of deformation twinning, J. Phys. Chem. Solids 25 (1964) 685–692, https://doi.org/10.1016/0022-3697(64)90177-5.

[73] M.J. Szczerba, M.S. Szczerba, Slip versus twinning in low and very low stacking-fault energy Cu-Al alloy single crystals, Acta Mater. 133 (2017) 109–119, https://doi.org/10.1016/j.actamat.2017.05.011.

[74] Y.Z. Tian, L.J. Zhao, S. Chen, A. Shibata, Z.F. Zhang, N. Tsuji, Significant contribution of stacking faults to the strain hardening behavior of Cu-15%Al alloy with different grain sizes, Sci. Rep. 5 (2015) 2–10, https://doi.org/10.1038/srep16707.

[75] T. Mori, H. Fujita, TWINNING DEFORMATION IN SINGLE CRYSTALS OF Cu-8 at% Al ALLOY, Trans. Jpn. Inst. Met. 18 (1977) 17–24, https://doi.org/10.2320/matertrans1960.18.17.

[76] F. Tranchant, J. Vergnol, J. Grilhé, Twinning in α Cu-A1 crystals: an instability of plastic flow. Strength Met. Alloy. (ICSMA 8), Pergamon, 1989, pp. 167–172, https://doi.org/10.1016/b978-0-08-034804-9.50021-8.

[77] J.W. Christian, S. Mahajan, Deformation twinning, Prog. Mater. Sci. 39 (1995) 1–157, https://doi.org/10.1016/0079-6425(94)00007-7.

[78] L. Li, Z. Chen, S. Kuroiwa, M. Ito, K. Kishida, H. Inui, E.P. George, Tensile and compressive plastic deformation behavior of medium-entropy Cr-Co-Ni single crystals from cryogenic to elevated temperatures, Int. J. Plast. 148 (2022), 103144, https://doi.org/10.1016/j.ijplas.2021.103144.

[79] S.F. Liu, Y. Wu, H.T. Wang, J.Y. He, J.B. Liu, C.X. Chen, X.J. Liu, H.T. Wang, Z. P. Lu, Stacking fault energy of face-centered-cubic high entropy alloys, Intermetallics 93 (2018) 269–273, https://doi.org/10.1016/j.intermet.2017.10.004.

[80] G. Laplanche, A. Kostka, C. Reinhart, J. Hunfeld, G. Eggeler, E.P. George, Reasons for the superior mechanical properties of medium-entropy CrCoNi compared to high-entropy CrMnFeCoNi, Acta Mater. 128 (2017) 292–303, https://doi.org/10.1016/j.actamat.2017.02.036.

[81] Y. Wang, B. Liu, K. Yan, M. Wang, S. Kabra, Y.L. Chiu, D. Dye, P.D. Lee, Y. Liu, B. Cai, Probing deformation mechanisms of a FeCoCrNi high-entropy alloy at 293 and 77K using *in situ* neutron diffraction, Acta Mater. 154 (2018) 79–89, https://doi.org/10.1016/j.actamat.2018.05.013.

[82] N.L. Okamoto, S. Fujimoto, Y. Kambara, M. Kawamura, Z.M.T. Chen, H. Matsunoshita, K. Tanaka, H. Inui, E.P. George, Size effect, critical resolved shear stress, stacking fault energy, and solid solution strengthening in the CrMnFeCoNi high-entropy alloy, Sci. Rep. 6 (2016) 1–10, https://doi.org/10.1038/srep35863.

[83] P.R. Thornton, T.E. Mitchell, Deformation twinning in alloys at low temperatures, Philos. Mag. 7 (1962) 361–375, https://doi.org/10.1080/14786436208212171.

[84] O. Vöhringer, Der einfluss von legierungsart und konzentration auf die streckgrenze von α -kupferlegierungen, Z Für Met. 65 (1974) 352–358.

[85] G. Laplanche, A. Kostka, O.M. Horst, G. Eggeler, E.P. George, Microstructure evolution and critical stress for twinning in the CrMnFeCoNi high-entropy alloy, Acta Mater. 118 (2016) 152–163, https://doi.org/10.1016/j.actamat.2016.07.038.
[86] H. Suzuki, C.S. Barrett, Deformation twinning in silver-gold alloys, Acta Metall 6 (1958) 156–165, https://doi.org/10.1016/0001-6160(58)90002-6.
[87] L. Rémy, A. Pineau, B. Thomas, Temperature dependence of stacking fault energy in close-packed metals and alloys, Mater. Sci. Eng. 36 (1978) 47–63, https://doi.org/10.1016/0025-5416(78)90194-5.
[88] D. Molnár, X. Sun, S. Lu, W. Li, G. Engberg, L. Vitos, Effect of temperature on the stacking fault energy and deformation behaviour in 316L austenitic stainless steel, Mater. Sci. Eng. A 759 (2019) 490–497, https://doi.org/10.1016/j.msea.2019.05.079.
[89] M. Schneider, G. Laplanche, Effects of temperature on mechanical properties and deformation mechanisms of the equiatomic CrFeNi medium-entropy alloy, Acta Mater. 204 (2021), 116470, https://doi.org/10.1016/j.actamat.2020.11.012.
[90] B. Neding, O.I. Gorbatov, J.-C.C. Tseng, P. Hedström, *In situ* bulk observations and ab initio calculations revealing the temperature dependence of stacking fault energy in Fe–Cr–Ni Alloys, Metall. Mater. Trans. A Phys. Metall. Mater. Sci. 52 (2021) 5357–5366, https://doi.org/10.1007/s11661-021-06473-5.
[91] C. Wagner, A. Ferrari, J. Schreuer, J.P. Couzinié, Y. Ikeda, F. Körmann, G. Eggeler, E.P. George, G. Laplanche, Effects of Cr/Ni ratio on physical properties of Cr-Mn-Fe-Co-Ni high-entropy alloys, Acta Mater. 227 (2022), 117693, https://doi.org/10.1016/j.actamat.2022.117693.